Contributions of impurity band and electron-electron interactions to magnetoconductance in AlGaN

P. Tasli[a]; A. Yildiz[b]; M. Kasap[a]; E. Ozbay[cd]; S. B. Lisesivdin[a]; S. Ozcelik[a]

[a] Department of Physics, Faculty of Science and Arts, Gazi University, Teknikokular, 06500 Ankara, Turkey [b] Department of Physics, Faculty of Science and Arts, Ahi Evran University, Aşıkpaşa Kampüsü, 40040, Kırşehir, Turkey [c] Department of Physics, Bilkent University, Bilkent, 06800 Ankara, Turkey [d] Department of Electrical and Electronics Engineering, Bilkent University, Bilkent, 06800 Ankara, Turkey

First published on: 30 June 2010

PLEASE SCROLL DOWN FOR ARTICLE

Contributions of impurity band and electron–electron interactions to magnetoconductance in AlGaN

P. Tasli[a], A. Yildiz[b]*, M. Kasap[a], E. Ozbay[cd], S.B. Lisesivdin[a] and S. Ozcelik[a]

[a]*Department of Physics, Faculty of Science and Arts, Gazi University, Teknikokular, 06500 Ankara, Turkey;* [b]*Department of Physics, Faculty of Science and Arts, Ahi Evran University, Aşıkpaşa Kampüsü, 40040, Kırşehir, Turkey;* [c]*Department of Physics, Bilkent University, Bilkent, 06800 Ankara, Turkey;* [d]*Department of Electrical and Electronics Engineering, Bilkent University, Bilkent, 06800 Ankara, Turkey*

Low temperature electrical measurements of conductivity, the Hall effect and magnetoconductance were performed on a degenerate AlGaN sample. The sample exhibited negative magnetoconductance at low magnetic fields and low temperatures, with the magnitude being systematically dependent on temperature. The measured magnetoconductance was compared with models proposed previously by Sondheimer and Wilson [Proc. R. Soc. Lond. Ser. A 190 (1947) p. 435] and Lee and Ramakrishan [Rev. Mod. Phys. 57 (1985) p. 287]. Data were analyzed as the sum of the contribution of a two-band and electron–electron interactions to the magnetoconductance, applying these models to describe the observed behavior. Least-squares fits to the data are presented. In the sample, magnetoconductance can be explained reasonably well by assuming these contributions to the measured magnetoconductance. It was found that theoretical and experimental data were in excellent agreement.

Keywords: electron–electron interactions; two-band model; negative magnetoconductance; impurity band; AlGaN; MOCVD

1. Introduction

Wide band gap nitride semiconductors have recently been the subject of both theoretical and experimental interest [1–10]. In particular, ternary AlGaN is becoming increasingly important in optoelectronic and electronic devices, such as high electron mobility transistors (HEMTs) [3–8]. Electronic transport in AlGaN has been targeted for extensive studies due to its interesting electrical properties and possible technological applications. Efforts have been made by our team to find the correct electronic transport mechanism in AlGaN at different temperature ranges [5–8]. Previous studies failed to clarify the mechanisms of conduction in highly degenerate AlGaN at low temperatures. The highly degenerate state is observed with increasing carrier concentration in AlGaN and, in such cases, various disordered states arise in the structure [3–5]. The realization of n-type AlGaN with very high

---

electron concentrations provides an experimental basis for investigating in detail the role of disorder at low temperatures.

Key factors influencing degeneracy in AlGaN can be directly investigated via magnetoconduction (MC) measurements. Despite progress using these measurements in recent years, significant work is needed to further improve our understanding of the role of disordered states in this material. Studying MC in detail provides important insights into low temperature electron transport properties.

MC is frequently observed in degenerate systems and is governed by quantum corrections to the Drude conductivity (σ_0) [11]. These corrections generally originate from weak localization (WL) and electron–electron interactions (EEI) [11]. Such quantum corrections to the classical Boltzmann contribution of electrical conductivity are especially required in disordered systems at low temperatures. Since these effects can significantly modify electrical transport, their existence should be considered in the design of AlGaN-based devices.

Here, we report magnetotransport measurements on degenerate AlGaN and demonstrate that negative MC appears in nonmagnetic AlGaN.

2. Experimental

The n-$Al_{0.57}Ga_{0.43}N$/AlGaN/AlN structures were grown on *c*-plane [0001] Al_2O_3 substrates in a low-pressure MOCVD reactor. Prior to epitaxial growth, Al_2O_3 substrates were nitridated by exposing them to a NH_3 flow of 1000 sccm at 790 °C. After nitridation, 50 nm thick AlN nucleation layers were grown at the same temperature, followed by 140 nm high-temperature undoped AlN buffer layers at a temperature of 1075 °C, then, 140 nm thick undoped AlGaN and 340 nm thick Si-doped AlGaN layers. All layers, except the final AlGaN layer, were nominally undoped.

The Al mol fraction of the AlGaN layers was determined by implementation of Bragg's law using high-resolution X-ray diffraction (HRXRD results. HRXRD measurements were taken with a D8-Discover diffractometer equipped with a monochromator with four Ge (220) crystals for a Cu Kα1 X-ray beam ($\lambda = 1.5406$ Å).

For resistivity and Hall effect measurements via the van der Pauw method, a square ($5 \times 5 \, mm^2$) sample was prepared with four contacts at the corners. Using annealed indium dots, ohmic contacts to the sample were prepared and their ohmic behavior confirmed by current–voltage characteristics. Measurements were made at temperature steps over the range 35–100 K using a Lakeshore Hall effect measurement system (HMS). At each temperature step, the Hall coefficient (with maximum 5% error) and resistivity (with maximum 0.2% error in the studied range) was measured for both current directions, both magnetic-field directions perpendicular to the surface and all possible contact configurations between 0 and 1.4 T (with 0.1% uniformity).

3. Results and discussion

Hall effect measurements showed that the film was n-type. The carrier concentration *n* was nearly independent of temperature ($n = 1.1 \times 10^{19} \, cm^{-3}$). To gain a deeper
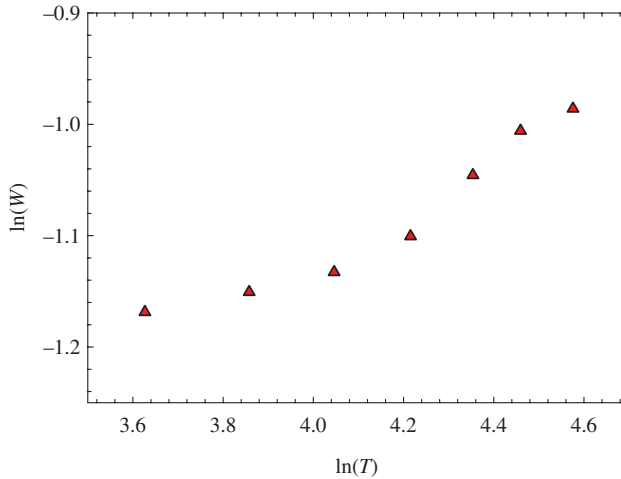
Figure 1. Plot of $\ln(W)$ versus $\ln(T)$ for AlGaN.

understanding, the conductivity behavior of the sample, a reduced activation energy plot was considered, as suggested by Zabrodskii and Zinoveva [12]:

$$W(T) = \mathrm{d}\left[\ln \sigma(T)\right]/\mathrm{d}[\ln(T)]. \tag{1}$$

According to the classification scheme on Zabrodskii and Zinoveva [12], when the slope of $\ln(W(T))$ versus $\ln(T)$ is negative, the sample is insulating; whereas a positive slope indicates a metallic sample. Figure 1 shows the plot of $\ln(W)$ versus $\ln(T)$ for the sample. Here, therefore, the investigated sample is metallic.

Figure 2 shows the temperature dependence of electrical conductivity in the range 35–100 K. Electrical conductivity linearly increases with $T^{1/2}$, which is in good agreement with the theory introduced for the presence of EEIs [13]:

$$\sigma(T) = \sigma_0 + mT^{1/2}, \tag{2}$$

where the $mT^{1/2}$ term is a correction to zero-temperatue conductivity (σ_0) due to the EEI. Equation (2) is fitted to the conductivity data of the sample. The solid line in Figure 2 is the best fitted values, with $r^2 = 0.998$ ($r =$ correlation coefficient) [14], indicating a satisfactory fit. The best fit was obtained with the parameters given in Table 1. Similar temperature dependencies were also observed in other metallic systems and attributable to the effects of EEI [1,2,10,15].

To test the model for electrical transport, we measured the MC of the sample at low temperatures (Figure 3). MC in non-magnetic degenerate semiconductors can originate from several effects, including weak antilocalization (WAL), Lorentz force, EEI and WL [11,16,17]. The first three have a negative effect on MC, whereas WL results in positive MC.

With spin–orbit scattering on top of the valence band in the material, the WAL effect becomes important. However, spin–orbit scattering depends on the atomic number of the doping atom. If the impurity atoms are heavy atoms, spin–orbit scattering will contribute significantly to MC [16]; otherwise, the contribution of the
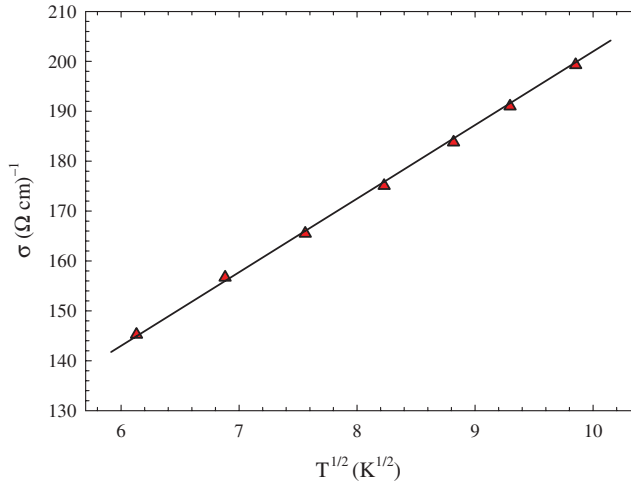
Figure 2. Variation in conductivity as a function of $T^{1/2}$ for AlGaN. Solid line is calculated using the least-squares technique.

Table 1. Physical parameter values of AlGaN.

Parameter	Value
σ_0 ($\Omega^{-1}\,\mathrm{cm}^{-1}$)	54.5
m ($\Omega^{-1}\,\mathrm{cm}^{-1}\,\mathrm{K}^{-1/2}$)	14.8
K (nm^{-1})	0.73
k_F (nm^{-1})	0.69
F_σ	0.44
l (nm)	1.39
D ($\mathrm{cm}^2\,\mathrm{s}^{-1}$)	1.01

Figure 3. Normalized MC $\left(\frac{\sigma(B)-\sigma(0)}{\sigma(B)}\right)\%$ at three temperatures for AlGaN. The solid lines represent the least-squares fit to Equation (21); symbols are experimental data.

WAL effect can be ignored. WAL produces a decrease in the zero magnetic-field conductivity with increasing temperature.

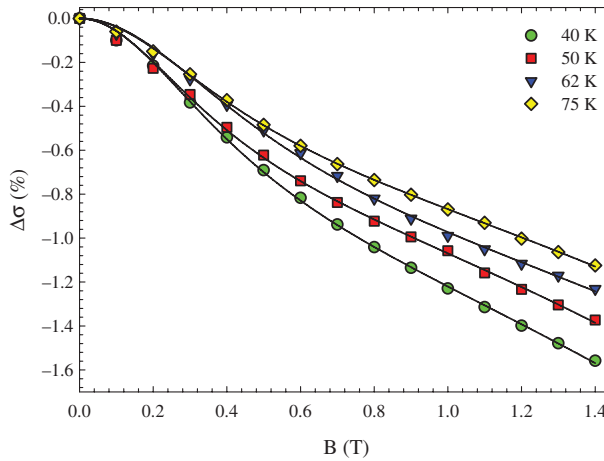MC resulting from Lorentz force can not be ruled out due to the presence of an impurity band in disordered semiconductor materials. The two-band model describes this effect [17]. The EEI effect involves modifications of effective Coulomb interactions in the presence of disorders in the systems [11]. It changes the density of states and, as a result, the zero magnetic field conductivity of the system increases with increasing temperature.

Since there is quantum interference between electronic waves at low temperatures, the probability of electron back-scattering is enhanced. This affects the WL of electrons, i.e. when an external magnetic field is applied, the WL is suppressed. Because the magnetic field suppresses wave coherence, quantum interference is reduced, resulting in positive MC [11]. The WL contributes to an increase in conductivity with increasing temperature.

In our case, since the MC is negative, as can be seen from Figure 3, the contribution of WL can be ruled out. MC data show no trace of spin–orbit interaction; therefore, the WAL effect can also be neglected. The presence of EEI was previously confirmed by fitting Equation (1) to zero field conductivity data of the sample. Since the formation of an impurity band in the sample is expected due to structural defects [3–5], the contribution of the Lorentz force to MC also has to be considered. To theoretically determine these two contributions to MC, we first deal with the EEI. Lee and Ramakrishnan [11] calculated the contribution of EEIs to MC in disordered metallic or highly degenerate systems using the following equations [11]:

$$\Delta\sigma = -Ag_3(h), \tag{3}$$

$$h = \frac{g\mu_B B}{k_B T}, \tag{4}$$

where g is the Landé factor ($g = 2$), k_B is Boltzmann's constant and μ_B is the Bohr magneton. The coefficient A is given by [11]

$$A = \frac{e^2}{4\pi^2\hbar}F_\sigma\left(\frac{k_B T}{2\hbar D}\right)^{1/2}, \tag{5}$$

where $\hbar$ is Planck's constant, e is the electron charge, D is the diffusion coefficient, and F_σ is related to the Fermi-liquid parameter F by [11,13]

$$F_\sigma = \left(\frac{-32}{3}\right)\left[1 - \frac{3F}{4} - \left(1 - \frac{F}{2}\right)^{3/2}\right]F^{-1}. \tag{6}$$

The value of F_σ ranges between 0 and 1 [13]. To calculate F_σ, Fermi-liquid parameter F is used as [11,13]

$$F = \frac{1}{x}\ln(1 + x) \tag{7}$$

$$x = \left(\frac{2k_F}{K}\right)^2, \tag{8}$$

where k_F is the Fermi wave vector given by

$$k_F = (3\pi^2 n)^{1/3};\tag{9}$$

the mean free path l of the carriers is also related to k_F by the expression

$$l = \frac{3\pi^2 \hbar \sigma_0}{e^2 k_F^2} = \frac{3m^* D}{\hbar k_F},\tag{10}$$

where n is the carrier density, ε is static dielectric constant and m^* is effective mass.

In Equation (8), K is the screening wave factor given as [11]

$$K = \left(\frac{12\pi n m^* e^2}{\varepsilon \hbar^2 k_F^2}\right)^{1/2}.\tag{11}$$

Ousset et al. [18] suggested suitable approximations for the function $g_3(h)$ in Equation (3):

$$g_3(h) \approx 5.6464 \times 10^{-2} h^2 - 1.4759 \times 10^{-3} h^4 + 4.2747 \times 10^{-5} h^6 \\ - 1.5351 \times 10^{-6} h^8 + 6 \times 10^{-8} h^{10} \quad h \leq 3\tag{12}$$

$$g_3(h) \approx 0.64548 + 0.235(h-4) - 7.45 \times 10^{-4}(h-4)^2 - 2.94 \times 10^{-3}(h-4)^3 \\ - 6.32 \times 10^{-4}(h-4)^4 - 5.22 \times 10^{-5}(h-4)^5 \quad 3 < h \leq 8\tag{13}$$

and

$$g_3(h) \approx h^{1/2} - 1.2942 - \frac{\pi^2}{12 h^{3/2}} - \frac{\pi^4}{16 h^{7/2}} - \frac{\pi^6}{32 h^{11/2}} \quad h > 8.\tag{14}$$

The limiting forms of $g_3(h)$ for large and small h are

$$g_3(h \to \infty) \approx \sqrt{h} - 1.3 \quad \text{and} \quad g_3(h \to 0) \approx 0.0565 h^2.\tag{15}$$

Next, we consider the the contribution of the Lorentz force to MC. Since the formation an impurity band in AlGaN is expected due to defects in its structure [3–5], we consider the contribution of the Lorentz force to the MC [17]:

$$\Delta\sigma/\sigma(0) = -\frac{a^2 B^2}{1 + b^2 B^2}.\tag{16}$$

Parameters a and b are functions of conductivity and the concentration of each group of carriers [16]:

$$a = \frac{\sqrt{\sigma_0}}{e}\left(\frac{\sigma_{01}}{n_1} + \frac{\sigma_{02}}{n_2}\right)\frac{\sqrt{\sigma_{01}\sigma_{02}}}{\sigma_{01} + \sigma_{02}}\tag{17}$$

$$b = \frac{1}{e}\left(\frac{n_1 - n_2}{n_1 n_2}\right)\frac{\sigma_{01}\sigma_{02}}{\sigma_{01} + \sigma_{02}},\tag{18}$$

where n_1 and n_2 are the carrier concentrations in different bands, and σ_{01} and σ_{02} are the conductivities for each group of carriers.

Normally, we could estimate a and b from Hall effect data in terms of the temperature-dependent carrier concentration and mobility data. Impurity-band effects are obvious at lower temperatures and are modeled by a simple, two-band approximation [19]:

$$\mu = \frac{n_1 \mu_1^2 + n_2 \mu_2^2}{n_1 \mu_1 + n_2 \mu_2} \qquad (19)$$

$$n = \frac{(n_1 \mu_1 + n_2 \mu_2)^2}{n_1 \mu_1^2 + n_2 \mu_2^2}. \qquad (20)$$

To obtain n_1, n_2, μ_1 and μ_2, Equations (19) and (20) must be fitted to the experimental data. Using the relation $\sigma = en\mu$, we could also determine σ_1 and σ_2, and then a and b. However, this involves an analysis of Hall data obtained at high temperature [20]. However, in the studied temperature range, the Hall data approached degeneracy and, therefore, we are unable to determine a and b independently from magnetic field data. High temperature analysis is not within the scope of this study, which deals with low-temperature magnetoconductance only.

Finally, the experimental MC data of the sample were analyzed as the sum of the EEI and Lorentz force contributions by applying an expression to describe the observed behavior. According to the Equation (15), MC will show an B^2 dependence at low magnetic fields and an $B^{1/2}$ dependence at high magnetic fields. In the range of the analyzed fields ($B = 0$–1.4 T) and temperatures ($T = 35$–100 K), $h \to 0$. Since $h \to 0$, least-squares fits to our MC data are then performed using Equations (3) and (16):

$$\Delta\sigma = -0.0565 A \left(\frac{g \mu_B B}{k_B T} \right)^2 - \frac{a^2 B^2 \sigma(0)}{1 + b^2 B^2}. \qquad (21)$$

Figure 3 shows representative results of normalized MC measurements $\left(\frac{\sigma(B) - \sigma(0)}{\sigma(B)} \right)\%$ up to high fields of 1.4 T for the sample at various temperatures. As can be seen, MC is negative, but the magnitude decreases systematically with increasing temperature. Representative fits to our data are also presented in Figure 3 for the sample at various temperatures. Agreement of the least-square fits to the data is excellent for the sample and temperatures. Values of the fit parameters A, a, and b are collated in Table 2. The values for parameters a and b decrease with increasing temperature, matching the experimental data, as expected [17].

Knowing $n = 1.1 \times 10^{19}\,\mathrm{cm}^{-3}$, k_F is determined initially from the Equation (9). Then, by using an iterative method [21], the values of D and K for $Al_y Ga_{1-y}N$ alloys as a function of y ($y = 0.57$) can be evaluated from the Equations (10) and (11), respectively. Here, we use the values of effective masses $m^* = 0.22 m_0$ and $0.48 m_0$, and static dielectric constants of $\varepsilon = 10.4$ and 8.5 for GaN and AlN, respectively [21]. Now, the value of F_σ is calculated using Equations (6)–(8). These calculated parameters are given in Table 1 and are of the same order of magnitude as found in degenerate semiconductor systems [2,3]. The values of A can be theoretically calculated using Equation (5) for various temperatures. The satisfactory agreement between the calculated and fitted (experimental) value of A is clear from Table 2.

Table 2. Values of parameters a, b and A (A_{Fit}) to fit Equation (21) and the values of A (A_{Teo}) parameters calculated using Equation (5) for the sample at different temperatures.

T (K)	a	b	A_{Fit}	A_{Teo}
40	0.233	2.29	0.617	0.468
50	0.228	2.15	0.636	0.469
62	0.191	2.07	0.517	0.432
75	0.185	1.79	0.567	0.518

This finding confirms that electron–electron interactions (EEIs) are dominant in the sample.

4. Conclusions

We report electrical transport measurements on AlGaN grown by MOCVD. Experimental results unambiguously indicate that low-temperature transport in AlGaN is associated with EEIs. This follows primarily from the experimentally observed temperature dependence of conductivity, which varies linearly with $T^{1/2}$. Detailed analysis of low-field magnetotransport in the sample showed negative MC behavior, with a decrease of magnitude with increasing temperature, which was interpreted as a manifestation of EEIs. Two-band and EEI models were used to fit the data. An agreement between the temperature dependence of MC and the models was obtained.

References

[1] A. Yildiz, S.B. Lisesivdin, M. Kasap and M. Bosi, Solid State Commun. 149 (2009) p.337.
[2] A. Yildiz, S.B. Lisesivdin, P. Tasli, E. Ozbay and M. Kasap, Current Appl. Phys. 10 (2010) p.838.
[3] K.Y. Chen, C.T. Liang, N.C. Chen, P.H. Chang and C.A. Chang, Chin. J. Phys. 45 (2007) p.616.
[4] Z. Dziuba, M. Gorska1, J. Antoszewski, A. Babinski, P. Kozodoy, S. Keller, B. Keller, S.P. Den Baars and U.K. Mishra, Appl. Phys. A 72 (2001) p.691.
[5] S.B. Lisesivdin, A. Yildiz, S. Acar, M. Kasap, S. Ozcelik and E. Ozbay, Physica B 399 (2007) p.132.
[6] S.B. Lisesivdin, N. Balkan, O. Makarovsky, A. Patanè, A. Yildiz, M.D. Caliskan, M. Kasap, S. Ozcelik and E. Ozbay, J. Appl. Phys. 105 (2009) p.093701.
[7] S.B. Lisesivdin, S. Demirezen, M.D. Caliskan, A. Yildiz, M. Kasap, S. Ozcelik and E. Ozbay, Semicond. Sci. Tech. 23 (2008) p.095008.

[8] S.B. Lisesivdin, A. Yildiz, S. Acar, M. Kasap, S. Ozcelik and E. Ozbay, Appl. Phys. Lett. 91 (2007) p.102113.

[9] A. Yildiz, F. Dagdelen, S. Acar, S.B. Lisesivdin, M. Kasap, Y. Aydogdu and M. Bosi, Acta Phys. Pol. (a) 113 (2008) p.731.

[10] A. Yildiz, S.B. Lisesivdin, S. Acar, M. Kasap and M. Bosi, Chin. Phys. Lett. 24 (2007) p.2930.

[11] P.A. Lee and T.V. Ramakrishnan, Rev. Mod. Phys. 57 (1985) p.287.

[12] A.G. Zabrodskii and K.N. Zinoveva, Phys. JETP 59 (1984) p.425.

[13] B.L. Altshuler and A.G. Aronov, in *Electron–Electron Interactions in Disordered Systems*, A.L. Efros and M. Pollak, eds., North-Holland, New York, 1985.

[14] R. Peck, C. Olsen and J. Devore, *Introduction to Statistics and Data Analysis*, Cengage Learning, London, 2009.

[15] K. Lal, A.K. Meikap, S.K. Chattopadhyay, S.K. Chatterjee, M. Ghosh, A. Barman and S. Chatterjee, Solid State Commun. 113 (2000) p.533.

[16] R. Meseryev and P.M. Tedrow, Phys. Rev. Lett. 41 (1978) p.805.

[17] E.H. Sondheimer and A.H. Wilson, Proc. R. Soc. Lond. Ser. A 190 (1947) p.435.

[18] J.C. Ousset, S. Askenazy, H. Rakoto and J.M. Broto, J. Phys. 46 (1985) p.2145.

[19] D.C. Look and R.J. Molnar, Appl. Phys. Lett. 70 (1997) p.3377.

[20] A. Yildiz, S.B. Lisesivdin, H. Altuntas, M. Kasap and S. Ozcelik, Physica B 404 (2009) p.4202.

[21] H. Morkoç, *Nitride Semiconductors and Devices*, Springer, Heidelberg, 1999.